ChemComm

A p-Type PbS Quantum Dot Ink with Improved Stability for Solution Processable Optoelectronics

Journal:	*ChemComm*
Manuscript ID	CC-COM-06-2021-003014
Article Type:	Communication

COMMUNICATION

A *p*-Type PbS Quantum Dot Ink with Improved Stability for Solution Processable Optoelectronics

Received 00th January 20xx,
Accepted 00th January 20xx

DOI: 10.1039/x0xx00000x

Fiaz Ahmed, [a] John H. Dunlap, [a] Perry Pellechia [a] and Andrew B. Greytak *[a]

Abstract: A highly stable *p*-type PbS-QDs ink is prepared using a single-step biphasic ligand exchange route, overcoming instability encountered in previous reports. Chemical characterization of the ink reveals 3-mercaptopriopionic acid (MPA) capped QDs stable in benzylamine solvent over a period of weeks or longer. The film resistivity, 1.45 kΩ-cm, is an order magnitude lower, and surface roughness ~ 0.5 nm is superior, *vs*. PbS films reported so far, and proof of concept photovoltaic devices showed efficiency >5.5%.

Colloidal quantum dots (QDs) are promising absorber materials for applications in optoelectronics and photovoltaic devices due to their tunable absorbance stemming from a size-dependent optical band gap that can be fine-tuned for solar energy capture. More importantly, these materials are compatible with low-temperature thin film solar concentrators, flexible and printable solar cells, and photodetectors manufacturable at industrial scales and at at low cost as compared to their crystalline-based counter parts[1–3]. To get the most power out of a solar cell device, tandem solar cells based on quantum dots is another approach that raises the possibility of increasing power conversion efficiency beyond the single junction limit[4].

In recent years, the efficiency of QD-based photovoltaic devices has improved significantly, with improvements in new device architectures, such as the quantum heterojunction devices, and the realization of improved ligand exchange and fabrication processes, including the introduction of n-type and p-type QD inks.[5,6] Record-setting QDs photovoltaic devices reported so far are fabricated using solid-state ligand exchange to replace long greasy aliphatic ligands used in the synthetic step.[7]

The solid-state film fabrication and ligand exchange (SSLE) technique is highly inefficient with dual drawbacks: it leads to waste of material as only about 1% of synthesized quantum dots end up being incorporated into the actual device, and is incompatible for large area application.[8,9] Additionally, the volume change associated with SSLE yields rough and cracked films following exchange treatments, and requires successive layers to fill the cracks and obtain smooth and continuous films. For these reasons, much attention has been given to solution-based ligand exchanged processes to formulate quantum dot inks that can be directly incorporated into devices through more conservative spray or roll-to-roll printing techniques for large area deposition for mass scale photovoltaic applications.

There are many reports in literature for solution-based halide ligand exchanged quantum dot inks forming *n*-type colloidal suspensions, but only a handful of publications focus on *p*-type quantum dot inks.[7,10–12] In SSLE work with PbS QDs, ethanedithiol (EDT) has been a benchmark ligand treatment for the formation of *p*-type films. Besides EDT, 3-mercaptopropionic acid (MPA) is the most explored and suitable organic ligand for PbS QDs to yield high-efficiency quantum dot solar cells through SSLE, as it can achieve a similar interparticle distance to EDT and maintains the thiol functional group.[13–15] MPA has also been a focus for development of PbS QD inks based on the hope that the carboxylic acid group can confer solubility in polar liquids through hydrogen bonding interactions and/or charge stabilization, but it has been challenging to find optimum solvent conditions for stabilizing such inks. For example, MPA-capped quantum dots have been dispersed in DMF or DMSO, but these solvents also interact with the PbS surface and MPA tends to form crystals in these solvents undermining their stability and subsequent device performance.[4,16] Recently, butylamine has been investigated as a solvent component for p-type inks, including butylamine-stabilized water-soluble MPA-capped QDs,[6] and hybrid inorganic/organic passivated PbS QDs in which the surface is initially treated with halides prior to thiolate ligand exchange.[7,17] Notably, this approach, combined with a SSLE-deposited PbS-EDT and hole transport layer, led to record performance for colloidal QD solar cells. Yet, butylamine can also etch QD surfaces, causing precipitation and loss of quantum confinement within hours[18], presenting concerns for manufacturing QD devices on a large scale and in a reproducible manner.[19] It is important to explore ligand and solvent chemistry for QD inks that can improve processability and device performance, also, to establish the nature and extent of ligand exchange that is occurring when such inks are prepared.

[a] *Department of Chemistry and Biochemistry, University of South Carolina, Columbia, South Carolina 29208, United States.*
[†] *Electronic supplementary information (ESI) available.*

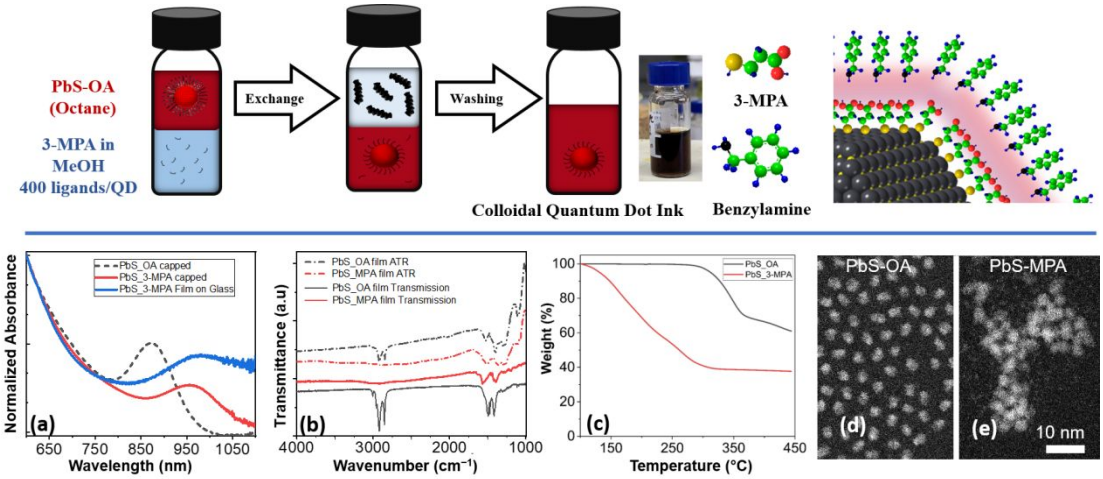

Fig. 1 (Top) biphasic ligand exchange process. (a) UV-Vis absorption spectra of pre- and post-ligand exchanged PbS QDs and PbS-MPA film on glass, normalized at 600 nm. Light scattering and dispersion contribute to the baseline absorption of the film. (b) FTIR absorption and attenuated total reflection spectra of films (c) thermogravimetric weight lose traces of PbS-OA and PbS-MPA QDs solids (e) STEM images of oleic acid and MPA capped PbS QDs.

Here, we report highly stable MPA-capped PbS QDs dispersed in benzylamine (BnzAm) through a rapid biphasic exchange technique using methanol (MeOH) as the ligand exchange solvent. We postulated that small, polar mercaptans can be paired with a suitably matched weakly-coordinating organic solvent. BnzAm is a less polar organic solvent that is also compatible with the rest of the device architecture. In addition, MeOH has the dual advantages of weaker interaction with the QD surface compared to DMF and a boiling point low enough compared to BnzAm that it can be effectively removed from the QD-MPA/BnzAm mixture under partial vacuum. We have performed comprehensive quantitative and qualitative analysis on the MPA-capped PbS quantum dot ink, and on photoconductive and photovoltaic test devices made using it. These devices are formed at ambient temperature using spin-coating, but the ink-based approach is highly suitable for making *p-n* junction and standalone heterojunction solar cell devices using a variety of methods including simple drop casting, and should be extensible to spray or roll to roll printing processes.

Ligand exchange and film deposition steps were conducted in a N_2-filled glovebox. A solution of MPA in MeOH was stirred with an oleate-capped PbS QD stock solution (880 nm peak absorbance, ~2.8 nm diameter, Fig. 1). After washing with *n*-octane to remove exchanged oleates from the system, the MPA-capped PbS QDs were precipitated from MeOH and BnzAm was added, forming a well-dispersed solution (details in ESI). In a control experiment, addition of butylamine failed to produce a stable colloidal solution (see ESI, Fig. S1), in agreement with previous observations[7]. Ultraviolet-visible-NIR absorbance spectra of the oleate-capped QDs in octane and of the ligand-exchanged PbS-MPA QD solution are shown in Fig. 1a. Both spectra show a distinct lowest-energy electronic excitation (exciton) peak. The presence of a well-defined absorbance peaks indicates retention of a narrow, quantum-confined size distribution, but a red shift is observed that we attribute primarily to extension of electron-hole pair's wavefunctions into the capping ligands.[20] The absorption spectrum of the QDs in the BnzAm scales linearly with concentration, and the QDs remained stable for weeks or more with no prominent change in spectrum and no significant light scattering, as illustrated in Supplementary Fig. S2. The exciton peak position is similar in films deposited from the ink (Fig. 1a).

Infrared spectroscopy (Fig. 1b) performed in attenuated total internal reflectance (ATR) and transmission modes showed that the C-H stretching peaks of oleate ligand around 3000cm^{-1} are absent in films deposited from the MPA-capped ink, indicating a complete ligand exchange. Ligand exchange was further investigated by thermogravimetric (TGA) analysis under inert (N_2) atmosphere. Fig. 1(c) presents the TGA from PbS-OA and PbS-MPA. The loss of ~30% of initial mass around 360°C is characteristic of OA-molecules attached to QD surface through carbonyl attachment[21]. In contrast, MPA gradually leaves the dried ink sample giving continuous mass loss until 250°C. This long TGA slope is attributed to the presence of strongly- and weakly-bound MPA in the sample, as is also evident from NMR experiments.

Scanning transmission electron microscopy (STEM) images displayed in Fig. 1 (d,e) revealed a significant decrease in the distance between neighboring MPA-capped particles deposited from the BnzAm ink compared to those with oleate capping, consistent with a ligand shell of smaller thickness, while the QDs retain a similar size distribution.

The ligand exchange process was further characterized by 1D ^{1}H NMR, and by diffusion ordered ^{1}H NMR spectroscopy (DOSY). Since a deuterated form of the benzylamine solvent was not easily available for this study, we performed NMR analysis in the natural abundance (proteo) solvent. In the 1D spectra in Fig. 2, no bound or free OA could be detected in the final ink solution (see also expanded spectra and reference oleic acid spectra in ESI, Figs. S3 and S4). On the other hand, the alkyl proton peaks of MPA in the QD-MPA sample (2 and 3, Fig. 2) are significantly broadened and shifted from those observed when MPA is added to clean BnzAm solvent in the absence of QDs.

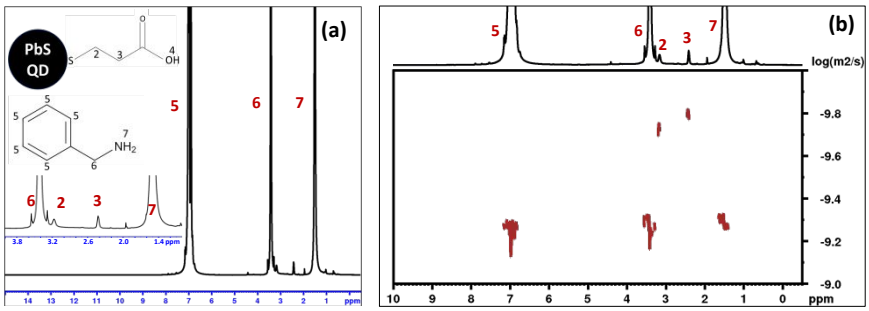

Fig. 2 (a) ^{1}H NMR spectrum of PbS-MPA in benzylamine. Inset: magnified scale revealing MPA methylene resonances. (b) Corresponding DOSY plot indicating slow effective diffusion constant for MPA interacting with the QD surface.

These shifts help in establishing the binding mode of MPA ligand. The broad signals at 2.42 and 3.17 ppm suggest that the MPA constitutes a single population that is strongly interacting with the QD surface on the NMR timescale. To further evaluate the extent of binding, we used a DOSY experiment with gradient pulse δ = 4 ms and diffusion period Δ = 25 ms. The MPA peaks in the QD sample indicate significantly slower diffusion compared to the benzylamine solvent, and compared to the value for the MPA in benzylamine on its own, while the solvent peaks are unchanged (see also SI Figs. S5-S7). The ratio of MPA diffusion constants, through the Stokes-Einstein relationship, gives an effective hydrodynamic diameter of 1.2 nm for MPA in the PbS-MPA ink (Table S1). This is less than expected for the QD diameter (2.8 nm, from sizing curve), indicating that the MPA ligand is in dynamic equilibrium between bound and free forms under the conditions studied.

In order to evaluate the film deposition conditions and basic electronic properties of PbS QD solids cast from the PbS-MPA ink, we formed two-terminal lateral transport devices on Si/SiO_2 substrates with pre-patterned Ti/Au (15 nm/25 nm thickness) bottom contacts defined by photolithography and formed by electron beam evaporation.

A low-speed spin coating method (detailed in ESI) was used to fabricate thin films for devices to characterize the material for electronic properties. The PbS-MPA film morphology was analyzed using scanning electron microscopy (SEM) (Fig. 3b) and atomic force microscopy (AFM) (Fig. 3a). The surface roughness and film thickness were measured through AFM. The films showed a very smooth surface (Fig. 3c) with a rms surface roughness of 0.5 nm that is superior to SSLE films reported so far.[22,23] Such a smooth film morphology reduces the possibility of current leakage in stacked vertical devices.[24] The intrinsic dark resistivity of the deposited PbS-MPA film was evaluated *via* the transfer length method (TLM), in which the resistance is measured between pairs of parallel electrodes with increasing distance between them. The method yields the sheet resistance from the slope of this line and, when multiplied by the measured film thickness, the bulk resistivity. For the device examined in Fig. 3e, with a film thickness of 170 nm, we calculated a bulk resistivity of 1.45±0.03 kΩ-cm. This is significantly lower than previous reported values for state-of-the-art EDT-capped SSLE films reported in literature.[25,26] Two terminal lateral devices with smaller active area as shown in Fig.3d were used for lateral photoconductivity measurements. The devices showed a linear current-voltage (*I-V*) relationship consistent with ohmic contact to the Au-electrodes as expected based on the TLM results. A significant increase in conductivity was observed when the devices were illuminated with visible or NIR light. Laser illumination at 444nm and 650nm were used to determine responsivities of 3.9mA/W and 3.7mA/W respectively, for a 200 µm×75 µm active area device at 10 V applied bias (Fig. 3f).

We formed heterojunction photovoltaic devices with a TiO_2 *n*-type component (Fig. 4). The devices were kept in a N_2-filled glove box overnight at ambient temperature for aging to remove any residual solvent trapped in QDs film before evaporating metal top contacts through a shadow mask We used pure Au top contacts to define devices with active areas of $2mm^2$ and $8mm^2$. A total of 12 similar devices were measured on four different substrates made at same time with similar deposition conditions. These devices were tested for power generation under AM 1.5G 100mW/cm^2 using a home built solar simulator which was calibrated using a standardized Newport photodetector for light intensity Current density-voltage (*J-V*). characteristics were recorded using Keithley 2636A source meter. The standout device had an efficiency of 5.53% with a fill factor of 50%. We emphasize that this result was achieved without any SSLE QD deposition steps, whereas some previous work on QD inks has employed a SSLE-deposited PbS/EDT layer as a hole transport layer. We achieved an even larger open

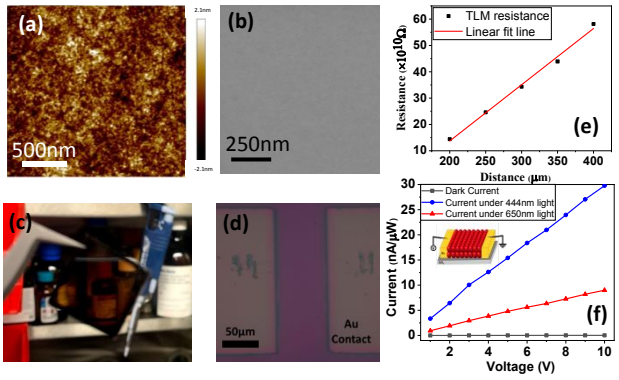

Fig. 3 (a) atomic force microscopy (AFM) (b) Scanning electron microscopy (SEM) images of surface morphologies of PbS-MPA film (c,d) optical image of film on glass and Si/SiO_2 substrate ((e) TLM measurement graph (f) dark and photocurrent under 560nm and 444nm laser light.

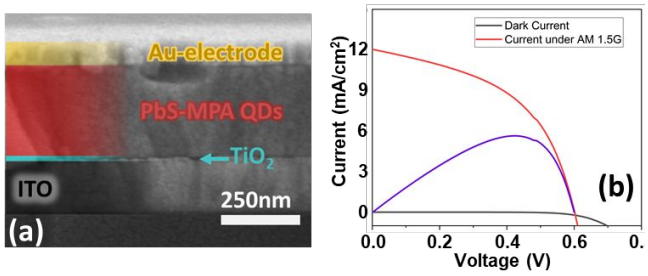

Fig. 4 (a) Heterojunction solar cell device architecture (b) cross-sectional SEM image of solar cell device (c) performance of the QD solar cell measured under AM 1.5G. The purple curve indicates the power on an arbitrary scale.

circuit voltage of 720 mV with an additional poly-TPD electron blocking/hole transport layer between the PbS QDs and the Au contact, but this caused the device efficiency to fall below 2%. While the efficiency stands the be improved with further optimization of device design, this open circuit voltage was on par to some of the highest reported V_{OC} for similar size quantum dots.

In summary we have synthesized a *p*-type PbS quantum dot ink using BnzAm as an organic ink solvent which is stable for several weeks under inert atmosphere. Benzylamine showed significantly greater solubility and stability of MPA-capped PbS QDs than did butylamine under identical conditions. We have demonstrated the applicability of this material in the fabrication of a heterojunction quantum dot solar cell with an efficiency over 5% under AM 1.5G radiation. Semiconductor inks are compatible with spin coating, spray coating and drop casting methods to make thick films for optoelectronic devices, especially solar cells. We note that the use of a low-boiling exchange solvent and higher-boiling ink carrier enables greater flexibility in formulation of the QD ink. For example, we have noticed that complete drying of the MPA-capped PbS QDs under vacuum, as might be required to remove a higher-boiling exchange solvent, can lead to difficulty in subsequent re-dispersion of the QDs. With MeOH as the exchange solvent, only gentle drying following exchange is necessary, and residual MeOH can be removed from the BnzAm solution under partial vacuum if desired. The character of the organic benzylamine solvent employed here raises the possibility of forming *p-n* junction type solar cells and detectors by incorporating solution-based *n*-type inks as well, and using printing or spray coating techniques to apply such materials to heat-sensitive flexible substrates.

This work was supported by the US NSF under Award CHE-1613388. JHD acknowledges an NSF IGERT fellowship under Award OIA-1250052. We thank Prof. Morgan Stefik for access to the solar simulator instrument, and Dr. Adam Roberge and Mathew L. Kelley for helpful discussions. We also thank Dr. Douglas Blom for assistance with STEM imaging.

Notes and references

1 E. H. Sargent, *Nature photonics*, 2012, **6**, 133–135.
2 J. Kim, O. Ouellette, O. Voznyy, M. Wei, J. Choi, M.-J. Choi, J. W. Jo, S.-W. Baek, J. Fan, M. I. Saidaminov, B. Sun, P. Li, D.-H. Nam, S. Hoogland, Z.-H. Lu, F. P. García de Arquer and E. H. Sargent, *Advanced Materials*, 2018, **30**, 1803830.
3 F. P. G. de Arquer, A. Armin, P. Meredith and E. H. Sargent, *Nature Reviews Materials*, 2017, **2**, 16100.
4 Y. Gao, J. Zheng, W. Chen, L. Yuan, Z. L. Teh, J. Yang, X. Cui, G. Conibeer, R. Patterson and S. Huang, *The journal of physical chemistry letters*, 2019, **10**, 5729–5734.
5 M. Liu, O. Voznyy, R. Sabatini, F. P. G. de Arquer, R. Munir, A. H. Balawi, X. Lan, F. Fan, G. Walters and A. R. Kirmani, *Nature materials*, 2017, **16**, 258–263.
6 H. Aqoma and S.-Y. Jang, *Energy & Environmental Science*, 2018, **11**, 1603–1609.
7 M.-J. Choi, F. P. G. de Arquer, A. H. Proppe, A. Seifitokaldani, J. Choi, J. Kim, S.-W. Baek, M. Liu, B. Sun and M. Biondi, *Nature Communications*, 2020, **11**, 1–9.
8 A. R. Kirmani, *MRS Bulletin*, 2019, **44**, 524–525.
9 H. Lee, H.-J. Song, M. Shim and C. Lee, *Energy & Environmental Science*.
10 J. Tang, K. W. Kemp, S. Hoogland, K. S. Jeong, H. Liu, L. Levina, M. Furukawa, X. Wang, R. Debnath and D. Cha, *Nature materials*, 2011, **10**, 765–771.
11 Z. Ning, H. Dong, Q. Zhang, O. Voznyy and E. H. Sargent, *ACS nano*, 2014, **8**, 10321–10327.
12 R. Wang, Y. Shang, P. Kanjanaboos, W. Zhou, Z. Ning and E. H. Sargent, *Energy & Environmental Science*, 2016, **9**, 1130–1143.
13 M. A. Zvaigzne, A. E. Aleksandrov, Y. Goltyapin, A. R. Tameev and A. A. Chistyakov, International Society for Optics and Photonics, 2018, vol. 10672, p. 1067235.
14 Z. L. Teh, R. J. Patterson, Z. Chen, Y. Gao, G. Conibeer and S. Huang, .
15 K. S. Jeong, J. Tang, H. Liu, J. Kim, A. W. Schaefer, K. Kemp, L. Levina, X. Wang, S. Hoogland and R. Debnath, *ACS nano*, 2012, **6**, 89–99.
16 C. C. Reinhart and E. Johansson, *Chemistry of Materials*, 2015, **27**, 7313–7320.
17 M. Gu, Y. Wang, F. Yang, K. Lu, Y. Xue, T. Wu, H. Fang, S. Zhou, Y. Zhang and X. Ling, *Journal of Materials Chemistry A*, 2019, **7**, 15951–15959.
18 R. Sliz, M. Lejay, J. Z. Fan, M.-J. Choi, S. Kinge, S. Hoogland, T. Fabritius, F. P. García de Arquer and E. H. Sargent, *ACS nano*, 2019, **13**, 11988–11995.
19 D. Bederak, N. Sukharevska, S. Kahmann, M. Abdu-Aguye, H. Duim, D. N. Dirin, M. V. Kovalenko, G. Portale and M. A. Loi, *ACS applied materials & interfaces*, 2020, **12**, 52959–52966.
20 C. Giansante, I. Infante, E. Fabiano, R. Grisorio, G. P. Suranna and G. Gigli, *Journal of the American Chemical Society*, 2015, **137**, 1875–1886.
21 A. Roberge, J. H. Dunlap, F. Ahmed and A. B. Greytak, *Chemistry of Materials*.
22 A. Kiani, B. R. Sutherland, Y. Kim, O. Ouellette, L. Levina, G. Walters, C.-T. Dinh, M. Liu, O. Voznyy and X. Lan, *Applied Physics Letters*, 2016, **109**, 183105.
23 R. T. Hickey, E. Jedlicka, B. S. S. Pokuri, A. E. Colbert, Z. I. Bedolla-Valdez, B. Ganapathysubramanian, D. S. Ginger and A. J. Moulé, *Organic Electronics*, 2018, **54**, 119–125.
24 L. Hu, R. J. Patterson, Y. Hu, W. Chen, Z. Zhang, L. Yuan, Z. Chen, G. J. Conibeer, G. Wang and S. Huang, *Advanced Functional Materials*, 2017, **27**, 1703687.
25 M. L. Kelley, J. A. Letton, G. Simin, F. Ahmed, C. A. Love-Baker, A. B. Greytak and M. V. S. Chandrashekhar, *ACS Applied Electronic Materials*.
26 E. J. Klem, H. Shukla, S. Hinds, D. D. MacNeil, L. Levina and E. H. Sargent, *Applied Physics Letters*, 2008, **92**, 212105.